Structure of the states of exciton-impurity and multiexciton-impurity complexes on nitrogen impurities in β-SiC

V. D. Kulakovskiĭ and V. A. Gubanov

Institute of Solid State Physics, Academy of Sciences of the USSR

T. G. Shevchenko State University, Kiev

(Submitted 30 July 1984)
Zh. Eksp. Teor. Fiz. **88**, 937–958 (March 1985)

We have investigated the emission spectra of β-SiC crystals doped with nitrogen impurities for different excitation densities for a wide range of temperature (2–50 K) and under conditions of uniaxial compression of the crystals along the [112] and [110] axes. We have determined the structure of the ground state and a series of excited states of the exciton-impurity complexes (EIC) bound to nitrogen impurities and the change in the structure resulting from a reduction in the band degeneracy under uniaxial compression of the crystals. It is shown that the lowest excited state of the EIC for the undeformed and the strongly uniaxially compressed crystals is the state with two Γ_1 electrons and a hole in the $2p$ state Γ_8 and Γ_5^8, respectively. It is found that the principal features of the multiexciton-impurity complexes (MEIC) are described within the framework of the shell model. In the undeformed crystals the ground states of the complexes with m excitons for $m < 4$ are $\{2\Gamma_1, (m-1)\Gamma_3; m\Gamma_8\}$, and the lowest excited states, in contrast to silicon, are not states with an excited electron, ($\{\Gamma_1, m\Gamma_3; m\Gamma_8\}$), but states with an excited hole in the $2p$ shell—$\{2\Gamma_1, (m-1)\Gamma_3; (m-1)\Gamma_8, (2p)\Gamma_8\}$. The ground state of the E_5IC is $\{2\Gamma_1, 4\Gamma_3; 4\Gamma_8, (2p)\Gamma_8\}$. The binding energies of the complexes have been determined. It is shown that the most important splitting of the one-electron states in the MEIC in undeformed SiC is caused by the electron-electron exchange for electrons, and this results in the splitting of the ground state in E_3IC (two Γ_3 electrons), and the electron-hole exchange of electrons with a $(2p)\Gamma_8$ hole. It is found that, in contrast to the case of MEIC in Si, when the degeneracy is lifted only in the valence band stable complexes with three bound excitons remain (the third hole goes into the $2p$ shell). When the degeneracy is lifted in both bands ($\mathbf{P} \| \langle 112\rangle$) as well, then, as in Si, only the ordinary EIC's remain stable.

§1. INTRODUCTION

The bound states of excitons and shallow impurities in semiconductors with an indirect band gap have a number of special features. In particular, there have been observed in these semiconductors multiexciton-impurity complexes (MEIC) which do not have hydrogen molecule analogs.[1] Investigations of complexes bound to shallow donors and acceptors in silicon have shown that these features are primarily due to an additional degeneracy of the $1s$ states for the electrons and holes bound into the complexes, where this degeneracy is a result of the high degree of degeneracy of the electron and the hole bands.[2–4] Because of the relatively low symmetry of the impurity center (group T_d) the $1s$ states of the electrons on donors are split into symmetric (Γ_1) states and antisymmetric states (Γ_3 and Γ_5 in Si, which has six valleys, and only Γ_3 in β-Si, which has three valleys).[5] According to the shell model, which has been proposed for the description of multiexciton-impurity complexes (MEIC) by Kirchenov,[2] the electrons in the MEIC's occupy successively the one-electron states of the neutral donor while the holes occupy the hole shell having the symmetry of the valence band (Γ_8). There can be up to four holes in the Γ_8 shell. Nothing is presently known about the states that are occupied by the subsequent holes.[6] Such a one-electron shell model, in which the interparticle interactions are neglected, gives a satisfactory description of the MEIC's in silicon, where the fine structure of the states that is related to the interparticle interactions is observed in the spectrum only for high-quality crystals and with the use of high resolution spectral techniques.[7,8]

The structure of the emission spectra for both exciton-impurity complexes (EIC) and MEIC's in β-SiC crystals turns out to be more complex than in silicon.[6,9–11] A detailed analysis of the emission spectra of complexes in SiC has not yet been carried out. In Refs. 9–11 it was found that the intense emission lines in the no-phonon region of the spectrum correspond to the recombination of Γ_1 electrons with Γ_8 holes. The nature of the majority of the other emission lines for both EIC's and MEIC's remains unresolved. We note that the complex structure of the excited state spectrum of the EIC's has previously been observed in Ge crystals.[12] It was initially assumed that the structure was associated only with the interparticle exchange interaction in the excited state of the EIC $\{\Gamma_1, \Gamma_5; \Gamma_8\}$ (Refs. 12 and 13), but later it was found that in the lowest excited state the hole was found not in the $1s\Gamma_8$ shell, but in the $2p$ shell.[14] The origin of the other levels has not yet been clarified. From an experimental point of view the analysis of the excited state structure of the EIC's in SiC is considerably simpler because the binding energies of the EIC's are an order of magnitude greater than in Ge. In particular, in the identification of a whole series of

 0038-5646/85/030550-14$04.00 © 1985 American Institute of Physics

excited states in β-SiC crystals it has proved possible to utilize an analysis of the associated emission line splitting resulting from uniaxial compression of the crystals.

We have investigated the emission spectra of EIC's bound to nitrogen impurities in β-SiC both for the case of no-phonon emission and with the emission of *TA* and *LA* phonons. The investigations were carried out over a wide range of temperature and excitation density for undeformed crystals (§3), and crystals weakly (§4) and strongly (§5) compressed along the [112] and [110] axes. The experimental method is described in §2. On the basis of the analysis carried out we were able to determine the nature of all the principal emission lines of the EIC's. In particular, it was determined that between the ground state ($\{2\Gamma_1; \Gamma_8\}$) and the first electron-excited state ($\{\Gamma_1, \Gamma_3; \Gamma_9\}$) there are two states with *p*-type holes. Upon uniaxial compression of the crystals, the lower of these states tracks with the lower of the hole terms split off from the $1s\Gamma_8$ and the upper state tracks with the upper of the latter levels. The EIC's have electron states (Γ_1, Γ_3) (§3 and 4) that are analogous to the excited $2p$ hole states. In the crystals that are strongly compressed along the $\langle 112 \rangle$ axis by the lifting of the degeneracy on both bands, all the electron-excited states completely disappear, whereas the hole-excited states partially remain (§5).

The investigation of multiexciton-impurity complexes in β-SiC crystals is treated in §6. The structure of the MEIC's with 2–4 bound excitons is similar to that of MEIC's on neutral donors in Si. From the analysis of the emission of a five-exciton-impurity complex E_5IC it was found that the fifth hole in this complex is in the $2p$ state Γ_8, where, because of the small energy spacing between the $1s\Gamma_8$ and $2p\Gamma_8$ shells, the binding energy of the five-exciton complex turns out to be even larger than that of the four-exciton complex E_4IC in spite of the fact that a new shell is beginning to be filled. There is a great deal of interest in the analysis of the fine structure of the complexes that is caused by the interparticle interaction. It is found that the most important interaction in the undeformed crystals is the electron-electron interaction in the unfilled shell Γ_3. This interaction causes a splitting of about ~ 0.8 meV in the three- and four-exciton complexes. Moreover, it is found that the electron-hole exchange in the $2p$ state leads to a marked splitting in the one-electron states in the MEIC's.

§2. EXPERIMENTAL METHOD

In this investigation we studied single crystals of cubic SiC, grown from the gas phase, and with a nitrogen impurity concentration of 10^{15}–10^{16} cm^{-3}. The starting crystals were in the shape of thin (~ 0.1 mm) hexagonal plates with (111) faces. For the uniaxial compression experiments these crystals were cut into rectangular prisms of dimensions $2\times 3\times 0.1$ mm, and were oriented with the long edges along the [110] and [112] axes. The method of compressing the crystals uniaxially was similar to that used previously for Si crystals.[15] However, because the samples were very thin it was necessary to take special precautions to avoid bending them at the large deformations. This was achieved by very carefully controlling the translational motion of the plunger into the frame of the crystal deformation apparatus.

Unfortunately, under these conditions there was an unavoidable force of friction between the plunger and the frame amounting to several kg, and it was therefore not possible to determine the deformation of the crystal taking into account just the applied external force and the very small cross section of the samples. Therefore, in order to determine the deformation it was necessary to exploit the deformation dependence of some internal property of the crystal. To fit this role we have chosen the magnitude of the splitting of the hole term (Γ_8) (at low deformations) and the energy of the ground state of the EIC (at high deformations), these parameters depending linearly on the applied pressure in the corresponding regions of deformation.[11] For the case $\mathbf{P}\|\langle 111\rangle$ these dependences have been determined experimentally in Ref. 11. For $\mathbf{P}\|\langle 112\rangle$ we are unaware of such data. Therefore to determine the magnitude of P in this case we proceeded from the equality of the deformation potentials for $1s\Gamma_8$ holes in the EIC for the cases $\mathbf{P}\|\langle 110\rangle$ and $\mathbf{P}\|\langle 112\rangle$. Because of the possible anisotropy of the deformation potential the values of P given above may be somewhat different from the true ones; however this has no effect on the physical results obtained, since in the interpretation we use only the linearity of the scale of the applied pressure.[16]

The samples were placed in an optical thermostat, within which it was possible to maintain a temperature of from 1.7 K to 300 K. For temperatures $T \leqslant 4.2$ K the samples were placed directly in the liquid helium, while at higher temperatures they were placed in the helium vapor. The precision in the control of the temperature was 0.1 K.

For excitation of the crystals a continuous argon laser was used, ($\lambda = 488$ nm) with a power level up to 1 W. The spectral apparatus consisted of a double monochromator from a DFS-12 spectrometer having 600 lines/mm diffraction gratings and a dispersion of 5 Å/mm. The recombination radiation was detected with an FEU-79 photomultiplier, equipped to operate in the photon counting mode.

§3. STRUCTURE OF EXCITON-IMPURITY COMPLEX LEVELS IN UNDEFORMED CRYSTALS

Figure 1 shows the spectra of the emission of β-SiC crystals for relatively low excitation density and $T = 1.8$–30 K. The components corresponding to the recombination of electron-hole pairs without the participation of phonons (*NP*) as well as with the emission of *TA* phonons are shown. The number of lines in the *NP* component is considerably less than in the *TA* component. This difference is typical of indirect transitions in semiconductors and is due to the fact that the matrix element for transitions with the participation of a phonon is proportional to $M_{TA} \sim \int f_e(r) f_h(r) d^3r$, while for the no-phonon transitions it is determined by the short-range components of the impurity potential: $M_{NP} \sim f_e(0) f_h(0)$.[16] Here $f_e(r)$ and $f_h(r)$ are, respectively, the wave functions of an electron and a hole in the complex. Keeping in mind the difference in the structures of the matrix elements M_{NP} and M_{TA} we can, on the basis of the components of the *TA* and *NP* emission spectra, conclude that the lines α, γ, and $Z_{1,2}$, which are observed in the no-phonon

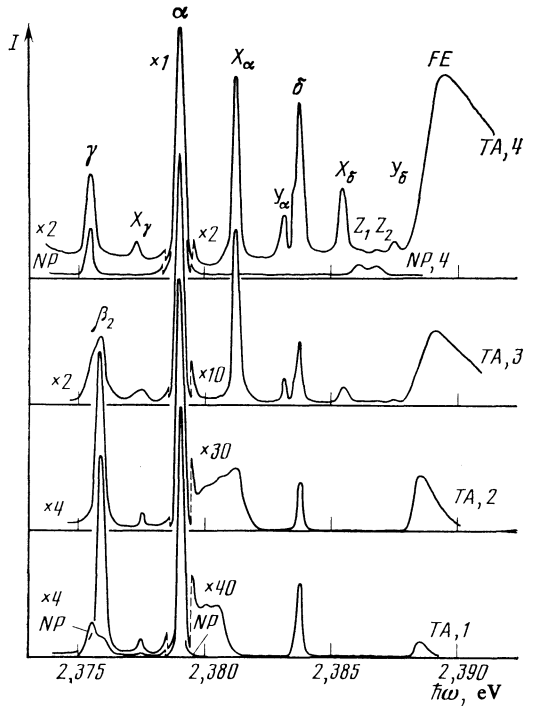

FIG. 1. Emission spectra of β-SiC for various temperatures at $W = 20$ W/cm^2 without phonon emission (NP) and with the emission of TA phonons (TA). For the TA spectra the horizontal axis gives the total energy of the photon and the TA phonon $\hbar\Omega_{TA} = 46.3$ meV. The curves 1) $T = 1.8$ K; 2) $T = 4.2$ K; 3) $T = 8$ K, and 4) $T = 24$ K.

spectrum, correspond to recombination of s electrons in the valley-symmetric state Γ_1 with s holes. The rest of the lines, which appear only in the phonon components, correspond to recombination of particles with extremely small values of $f_e(r)$ and (or) $f_h(r)$ for $r < a$, where a is the lattice constant. Among these in particular are the electron valley-antisymmetric states $1s\Gamma_3$ as well as the p states of the electrons and holes. We shall examine the nature of the observed emission lines individually.

The α line. The origin of this principal emission line of the EIC has been previously determined on the basis of magnetooptical and piezospectroscopic investigations.[11,9] It corresponds to the recombination of a $1s\Gamma_1$ electron with a Γ_8 hole in the ground state $\{2\Gamma_1; \Gamma_8\}$ of the EIC.

The β_2 line. The intensity of the β_2 line relative to that of α line decreases faster than linearly with decreasing excitation intensity. Below (§7) we shall show that this line corresponds to the recombination of an E_2IC.

The δ line. At high temperatures ($T = 15$–20 K) the ratio of the intensities of the δ to the α line is independent of the excitation density and is determined only by the temperature (Fig. 1). However, with decreasing temperature the ratio $I(\delta)/I(\alpha)$ begins to depend on the excitation density; it increases slightly with increasing W. For $T \leqslant 4.2$ K and large W the ratio of the intensities of the δ and α lines ceases to depend on the temperature and is determined only by the excitation density. The ratio of the δ and β_2 line intensities is found to be independent of the temperature and excitation density for $T < 4.2$ K and $W > 20$ W/cm^2. Therefore we associate the δ line with the recombination of an electron-hole pair in the excited state of the EIC which is the final state for the recombination of an electron-hole pair in an E_2IC. This state of the EIC is the electron-excited state $\{\Gamma_1, \Gamma_3; \Gamma_8\}$. The low temperature behavior of the δ line has a natural explanation if we assume that the time of radiative recombination of the EIC in this state is comparable to its relaxation time into the ground state of the EIC. This situation also occurs in the case of the EIC in silicon crystals.[16]

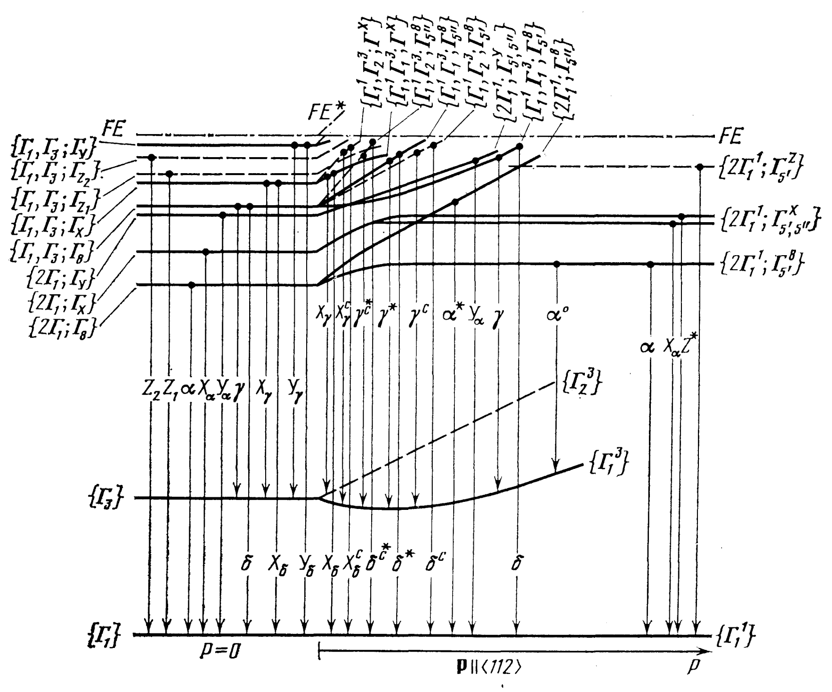

FIG. 2. Energy level diagram of EIC bound to a neutral donor (N) in undeformed and compressed along the ⟨112⟩ axis crystals of β-SiC. The arrows indicate the resolved transitions. $\Gamma_X \equiv \Gamma_{8'}$, $\Gamma_y \equiv \Gamma_{8''}$.

From the energy position of the δ line (above the line α), and taking into account the absence of the δ line in the no-phonon spectrum, we can conclude that this line corresponds to the transition $\{\Gamma_1, \Gamma_3; \Gamma_8\} \rightarrow \{\Gamma_1\}$ (Fig. 2).

The γ line. It is obvious that the δ line in the emission spectrum must be accompanied by another line associated with the recombination of an electron in the EIC: the transition $\{\Gamma_1, \Gamma_3; \Gamma_8\} \rightarrow \{\Gamma_3\}$. This line must be shifted toward the red from the δ line by the amount of the energy difference of the terms Γ_3 and Γ_1 of the nitrogen neutral donor, equal to 8.3 meV.[18] This line is actually observed in the emission spectrum of the EIC and it is the γ line. It is quite visible at temperatures above 10 K (Fig. 1). As expected, the ratio of the intensities of the γ and δ lines is independent of the temperature and the excitation density, and moreover, the γ line, which is associated with the recombination of a Γ_1 electron is, in contrast to the δ line, quite evident in the no-phonon spectrum (Fig. 1). We note that at low temperatures, because of the relatively large concentration of E_2IC's, and the small energy spacing between the γ and β_2 lines, the γ line in the *TA* component is lost in the background of the β_2 line. However, in the no-phonon region, because of the small probability of the no-phonon transitions $\{2\Gamma_1, \Gamma_3; \Gamma_8\} \rightarrow \{\Gamma_1, \Gamma_3; \Gamma_8\}$, the γ line is also visible at 2 K (Fig. 1).

Thus, from the spectral positions of the α, γ, and δ lines it follows that the lowest electron excited level in the EIC $\{\Gamma_1, \Gamma_3; \Gamma_8\}$ is located above the ground state by 4.8 meV.

The X_α and Y_α lines. The X_α and Y_α lines are located between the α and δ lines and are observed only in the phonon components (Fig. 1). These lines are practically invisible in the spectrum at 2 K, and they rise up rapidly with increasing temperature. From an analysis of the temperature dependences of the α, X_α and Y_α lines it follows that the energy of the energies of the EIC excited states, the recombination of which produces the X_α and Y_α lines, coincides with the energy spacings between these lines and the α line. These energies are less than the energy of the $\{\Gamma_1, \Gamma_3; \Gamma_8\}$ state. Therefore we assume that the X_α and Y_α lines are associated with the recombination of EIC's that in the excited state have only holes. In accord with this assumption, the X_α and Y_α lines do not have satellite lines similar to the γ and δ lines. Because the X_α and Y_α lines are absent from the no-phonon spectrum in spite of the recombination of an electron in the Γ_1 state, it must be assumed that the recombining hole is located in the $2p$ states Γ_X and Γ_Y. Thus, we associate the X_α and Y_α lines with the recombination of EIC's in the states $\{2\Gamma_1; \Gamma_X\}$ and $\{_2\Gamma_1; \{\Gamma_Y\}$ Additional arguments for this interpretation will be given in §4 in the analysis of the results of piezospectroscopic investigations.

The small difference in the energies of the hole states $1s\Gamma_8$ and $2p\Gamma_{X,Y}$ in EIC's bound to donors is evidently due to the fact that the self consistent potential for holes in EIC's bound to a donor becomes repulsive for $r \ll a$ because of the positive charge of the donor ion. Because of this the energy of the ground state, the slow wave function of which is a superposition of $1s$, $3d$, and $5g$ type hydrogen-like wave functions,[19,20] increases sharply. The perturbation of the $2p$ hole states, which are a mixture of $2p$ and $4f$ states,[19,20] and, consequently the energies of these states, are considerably lower because of the vanishing of the p and f functions at $r = 0$. Therefore the energy difference $\Delta_{s\text{-}p}$ between the $1s$ and $2p$ hole states in the EIC is considerably less than for the neutral acceptor. The $2p$ hole state in a field of tetrahedral symmetry is split into four states, $\Gamma_6 + \Gamma_7 + 2\Gamma_8$. Up to the present time observations have been reported of only one of the $2p$ hole states in the EIC bound to a neutral donor in Ge.[14] The value of $\Delta_{s\text{-}p}$ in Ge was found to be equal to $0.25\,R$, where R is the excitonic Rydberg. In β-SiC for the state Γ_X, $\Delta_{s\text{-}p} \approx 2.2$ meV or $\approx 0.08\,R$, while for the state Γ_Y the value of $\Delta_{s\text{-}p} \approx 0.14\,R$.

The X_γ, X_δ, and Y_δ lines. These lines we associate with the recombination of EIC's for which one of the electrons is in the excited state $1s\Gamma_3$ and the hole is in the excited p states Γ_X or Γ_Y. This interpretation is supported by the following facts. First, the difference in energy for the transitions X_δ–δ and Y_δ–δ are only slightly different (less) than the energy differences respectively for the transitions X_α–α and Y_α–α (Fig. 1). Second, from Fig. 1 it can be seen that these lines are observed only in the phonon replicas. Further, it has been determined experimentally that the intensity ratio of the X_γ and X_δ lines is independent of the temperature and the excitation density, i.e., these lines correspond to the recombination in the EIC of holes with electrons in different states. The energy difference for the transitions X_Y and X_δ is exactly equal to the energy difference of the states Γ_3 and Γ_1 of the neutral donor nitrogen–8.3 meV. It is therefore reasonable to assume that these lines correspond to transitions from the excited state $\{\Gamma_1, \Gamma_3; \Gamma_X\}$ of the EIC into the state $\{\Gamma_1\}$ (the X_δ line) and $\{\Gamma_3\}$ (the X_γ line) of the neutral donor (Fig. 2). From the state $\{\Gamma_1, \Gamma_3; \Gamma_Y\}$ two transitions Y_δ and Y_γ should also be observed, with an energy difference 8.3 meV (Fig. 2). However at this distance from the Y_δ line an intense EIC α emission line appears in the spectrum and it does not appear possible to separate the Y_γ line.

The Z_1 and Z_2 lines. These lines are quite visible at high temperatures in the non-phonon component of the spectrum and are almost unresolved out of the background of the more intense X_δ and Y_δ lines in the *TA* component. The large probability of the no-phonon transitions Z_1 and Z_2 indicates that they correspond to the recombination of s electrons in the Γ_1 state and holes that are most likely in s states. One of these states of the EIC may be $\{2\Gamma_1; (2s)\Gamma_8\}$, which is fourfold degenerate in the spin of the hole and should not be split in a field of tetrahedral symmetry. The nature of the second line is still not clear. To associate it with the recombination of a hole in a spin-orbit split state $1s\Gamma_6$, which in β-SiC is close to $1s\Gamma_8$ is not permitted on the one hand by the relatively low intensity of thse lines in the phonon region in comparison with the X_δ and the Y_δ lines, and on the other hand by the rather large difference between the spin-orbit splitting of the hole in the free exciton (10.36 meV, Ref. 21) and the energies of the states corresponding to the lines Z_1 (6.7 meV) and Z_2 (7.5 meV) (Fig. 1).

Further information on the structure of the excited levels of the EIC both in the undeformed and the uniaxially compressed β-SiC crystals can be obtained from piezospectroscopic measurements, which are the subject of the next section.

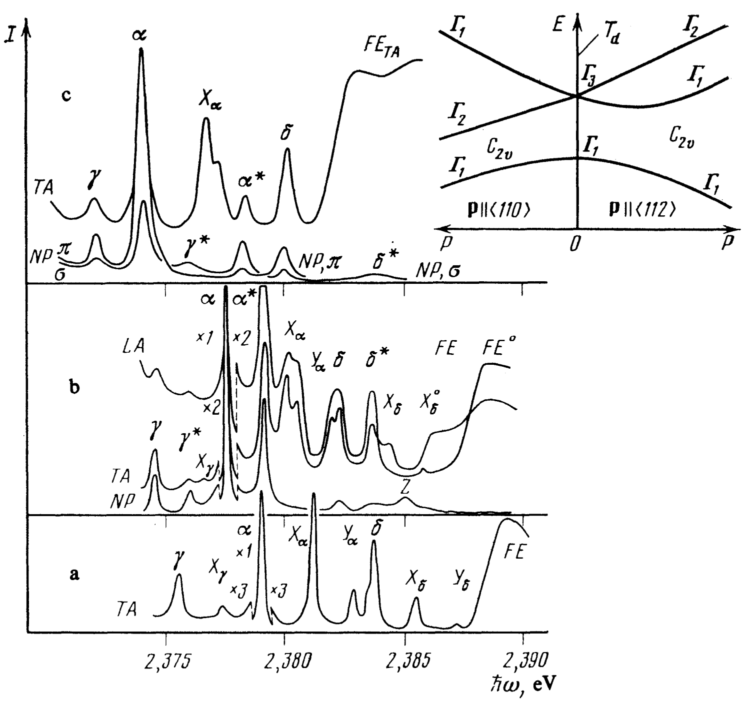

FIG. 3. Change in EIC emission spectra for uniaxial deformation of the crystals along the ⟨112⟩ axis, $T = 25$ K. For the *TA* and *LA* components of the spectrum the horizontal axis gives the total energy of the emitted photon and phonon. a) $P = 0$; b) $P = 130$ MPa; c) $P = 360$ MPa. The insert shows the splitting of the neutral donor levels due to compression of the β-SiC along the ⟨112⟩ and ⟨110⟩ axes.

§4. SPLITTING OF EIC LEVELS DUE TO UNIAXIAL COMPRESSION OF THE CRYSTALS

In the analysis of the structure of the states of the EIC in β-SiC the following directions of the axis of compression are of interest: [111] (reduces the degeneracy only in the valence band), [110] (in addition one of the (001) valleys is split), and [001] or [112] (only one (001) valley in the conduction band remains (Ref. 19)). From the thin platelets with (111) faces that we had we were able to cut samples for the piezospectroscopic measurements along the ⟨110⟩ and ⟨112⟩ axes. Upon compression along these axes the neutral donor state is $1s\Gamma_3$, which is valley-antisymmetric, is split into two states:

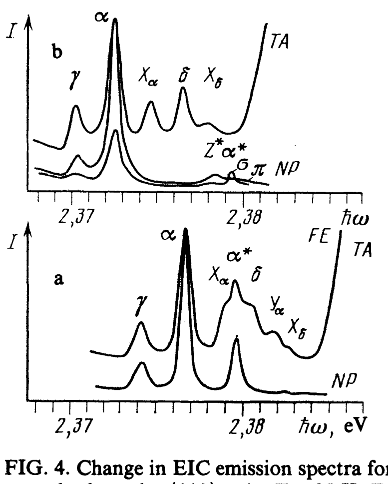

FIG. 4. Change in EIC emission spectra for uniaxial deformation of the crystals along the ⟨110⟩ axis, $T = 35$ K. For the *TA* components of the spectrum the horizontal axis gives the total energy of the emitted photon and phonon. a) $P = 200$ MPa; b) $P = 400$ MPa.

Γ_1^3 and Γ_2^3 (footnote 1), where for $\mathbf{P}\|\langle 111\rangle$ the lowest state is the antisymmetric state Γ_2^3, while for $\mathbf{P}\|\langle 112\rangle$ and $\mathbf{P}\|\langle 001\rangle$ it is the symmetric state Γ_1^3 (see the insert in Fig. 3).

Figures 3 and 4 show the no-phonon *TA* and *LA* components of the EIC emission spectra recorded for various deformations of the crystals along the ⟨112⟩ and ⟨110⟩ axes. On the basis of an analysis of the spectra we have generated a diagram of the splitting of the various emission lines of the EIC under these conditions (Fig. 5). We shall examine first the region of small deformations.

The EIC *ground state* $\{2\Gamma_1; \Gamma_8\}$, *the* α *line*. The splitting of this line into a doublet for $\mathbf{P}\|\langle 112\rangle$ and ⟨110⟩ is due to the splitting of the hole shell Γ_8, since the electron state Γ_1 is not split. In the no-phonon spectrum the short wavelength component of the α line has predominantly σ polarization (the electric field vector satisfies $\mathbf{E}\perp\mathbf{P}$, whle the long wavelength component has π polarization $\mathbf{E}\|\mathbf{P}$. It follows from this that the projection of the angular momentum of the hole in the split-off state is $\pm 3/2$ and $\pm 1/2$ in the ground state. Both of these states have Γ_5 symmetry, so we shall designate them $\Gamma_{5'}^8$ and $\Gamma_{5''}^8$, respectively.

EIC *electron-excited state* $\{\Gamma_1, \Gamma_3; \Gamma_8\}$, *the* γ *and* δ *lines*. The level $\{\Gamma_1, \Gamma_3; \Gamma_8\}$ in uniaxially compressed crystals is split into four levels as a result of the doublet splitting of the electron state Γ_3 and the hole state Γ_8 (Fig. 2). From Figs. 3–5 it can be seen that as expected the δ line, which corresponds to the recombination of a Γ_8 hole with a Γ_3 electron, is split into a quadruplet for $\mathbf{P}\|\langle 112\rangle$ and $\mathbf{P}\|\langle 110\rangle$. Because of the closeness of the Γ_3 electron and Γ_8 hole splitting, the two middle components are not resolved at small deformations. The γ line, which corresponds to the recombination of a Γ_1 electron and also the α line are split into a doublet, where the splitting of the γ and α lines are equal

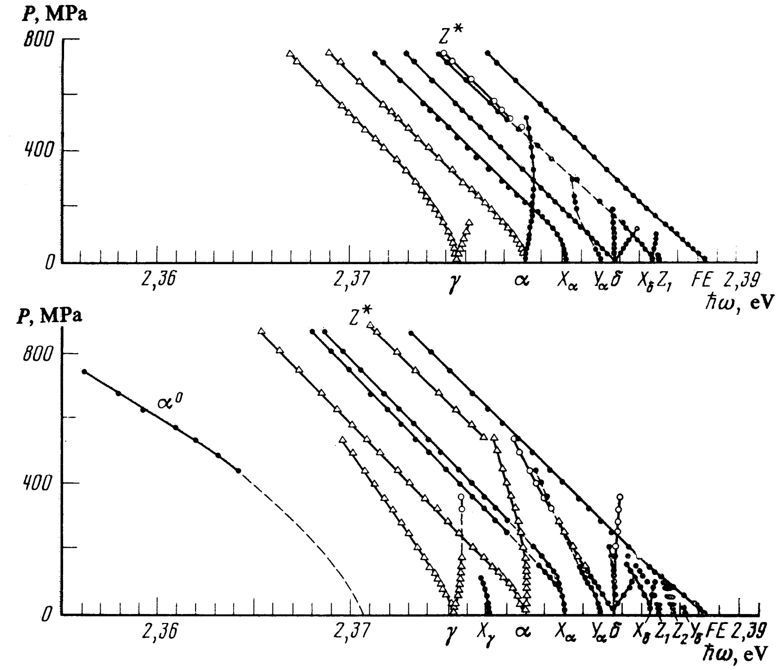

FIG. 5. Diagram of the splitting of the EIC emission lines for uniaxial compression along the ⟨110⟩ and ⟨112⟩ (below) axes. △) emission lines observed in *Np* and *TA* regions of the spectrum; ○) only in the *NP* region, ●) only in the *TA* region.

(Fig. 5). We note that the absence of additional splitting of the γ line indicates the closeness of the splitting of the Γ_3 electron term for an EIC and for a neutral donor. At large deformations the energies of the transitions $\{\Gamma_1^1, \Gamma_1^3; \Gamma_5^8\} \rightarrow \{\Gamma_1^3\}$ and $\{\Gamma_1^1, \Gamma_2^3; \Gamma_5^8\} \rightarrow \{\Gamma_2^3\}$ should be different because of the difference in the splitting of the Γ_2^3 and Γ_1^3 states for the neutral donor and the EIC. However, it is not possible to observe experimentally the splitting of the γ line because of the extremely low population of the upper electron state at large deformations.

In crystals that are compressed along the ⟨112⟩ axis the lower of the Γ_1^3 and Γ_2^3 electron states is Γ_1^3 and in crystals compressed along the ⟨110⟩ axis it is Γ_2^3 (Fig. 3). Therefore the behavior of the δ line in the no-phonon component of the spectrum in these two cases differ qualitatively: for $\mathbf{P}\|\langle 110\rangle$ the long wavelength component of the δ line is absent (as in the undeformed crystal), while for $\mathbf{P}\|\langle 112\rangle$ it increases sharply at large deformations.

Thus, the piezospectroscopic investigations fully support the proposed interpretation of the γ and δ lines

The excited hole states $\{2\Gamma_1; \Gamma_{X,Y}\}$ *of* EIC, *the* X_α *and* Y_α *lines.* The X_α line is quite far from neighboring lines and it was possible to trace its splitting up to the largest deformations (Figs. 3–5). For $\mathbf{P}\|\langle 112\rangle$ the X_α line is split into a doublet; the amount of its splitting is considerably smaller than that of the α line, and it saturates at very small deformations. Further, it can be seen from Fig. 5 that already at small deformations the X_α line intersects the short wavelength component of the α line. Neither of the components of the doublet X_α can be seen in the no-phonon spectrum either for $\mathbf{P}\|\langle 112\rangle$ or for $\mathbf{P}\|\langle 110\rangle$.

It is more complicated to follow the behavior of the Y_α line because of the proximity of the intense δ line. However, we can state that for both this line and the X_α line no splitting is observed that is comparable in magnitude to that of the $1s\Gamma_3$ electron term or the $1s\Gamma_8$ hole term. The Y_α line as well as the X_α line, both in the undeformed crystals and in uniaxially compressed crystals, are visible only in the phonon components. From Fig. 5 it can be seen that in the uniaxially compressed crystals the X_α line follows the long wavelength component of the emission line from the ground state of the EIC, while the Y_α component follows the short wavelength component. This behavior is clearly visible in the crystals compressed along the ⟨110⟩ axis, where the Y_α line at large deformations does not coincide in the spectrum with the δ line (Fig. 5).

The observed behavior of the X_α and Y_α lines under uniaxial compression of the crystals has a natural explanation within the framework of the interpretation proposed above, namely, the recombination of an EIC with a hole in excited $2p$ states. As already mentioned in §3, it follows from group theory that in undeformed crystals (field of tetrahedral symmetry) the $2p$ state is split into four, $\Gamma_6 + \Gamma_7 + 2\Gamma_8$; the levels Γ_6 and Γ_7 are doubly degenerate and the Γ_8 level is fourfold degenerate. The sequence of the levels is not predicted by group theory. As a result of the calculations of the energies of the excited $2p$ states of the EIC bound to donors in Si and Ge[20] it was found that in the crystals the lowest level is Γ_8 (the classification according to the O_h group within the framework of the effective mass approximation). The splitting of the X_α line due to uniaxial compression of the crystal indicates that in β-SiC also the lowest $2p$ level of the hole in the EIC bound to nitrogen is the Γ_8 level, since the twofold spin-degenerate states Γ_8 and Γ_7 are not split upon reducing the symmetry of the crystal to C_{2v}. We also note that while, in contrast to the case of the neutral acceptor, the states Γ_6 and Γ_7 in an EIC in an undeformed crystal would be practically unsplit, under uniaxial compression of the crystal their splitting should follow the splitting of the ground state of the hole ($1s\Gamma_8$). Taking into account this circumstance and bearing in mind that the energy differences of the lines X_α–α and Y_α–α are about the same for $\mathbf{P}\|\langle 110\rangle$ we propose that the Y_α line is also associated with the recombination of a hole in the Γ_8 state. Thus we identify the state $2p\Gamma_X$ with $2p\Gamma_8$ and $2p\Gamma_Y$ with $2p\Gamma_8$. The positions of the $\{2\Gamma_1; (2p)\Gamma_6\}$ and $\{2\Gamma_1; (2p)\Gamma_7\}$ levels of the EIC are still unclear. Here $\Gamma_{8'}$ and $\Gamma_{8''}$ are the two different superpositions of the $2p$ and $4f$ wave functions of the hydrogenic spectrum. We note that the sequence obtained for the hole $2p$ levels inthe EIC bound to donors, $\Gamma_{8'}$, $\Gamma_{8''}$, and $\Gamma_{6,7}$ agrees well with the known sequence[19,22,23] of the $2p$ levels of a hole bound to a neutral acceptor in Ge and Si, namely, $\Gamma_{8'}$, $\Gamma_{8''}$, Γ_7, and Γ_6.

We call attention to the fact that in the neutral acceptors that have been studied in Si and Ge it has been found that the splitting of the $2p$ states $\Gamma_{8'}$ and $\Gamma_{8''}$ in the region of small deformations is considerably less than that of the $1s\Gamma_8$ state and of the valence band. For instance, for B and Al in Si for $\mathbf{P}\|\langle 100\rangle$ the $2p\Gamma_8$ state is not split at all, while for $\mathbf{P}\|\langle 111\rangle$ its splitting is three times less that the splitting of the $1s\Gamma_8$ state. Thus, the behavior of the $2p$ hole states in an EIC bound to donors for very small deformations is in good qualitative agreement with the behavior of these states in the case of neutral acceptors. The region of large uniaxial deformations, where the $2p\Gamma^{8'}_{5''}$ level intersects the split-off $\Gamma^{8}_{5''}$ is level, has not been investigated experimentally in the neutral acceptor case because the energy diffference between the $1s\Gamma_8$ and $2p\Gamma_8$ terms for the neutral acceptor even in germanium requires a pressure $P > 1000$ MPa.

The higher excited state of the EIC $\{\Gamma_1, \Gamma_3; (2p)\Gamma_{8'}\}$, *the X_δ and X_γ lines*. Because of the small binding energy of this state the intensities of the X_δ and X_γ lines are small. Therefore it is possible to follow these lines only at rather small d formations. For both directions of crystal deformation the X_δ line (the transitions $\{\Gamma_1, \Gamma_3; (2p)\Gamma_8\} \rightarrow \{\Gamma_1\}$) is split only into a doublet, with a splitting equal to the splitting of the electron term Γ_3 of $\{\Gamma_1, \Gamma_3; (1s)\Gamma_8\}$ in the EIC, while the X_γ line (the transition $\{\Gamma_1, \Gamma_3; (2p)\Gamma_8\} \rightarrow \{\Gamma_3\}$ is not split at all (Fig. 5). This result is in agreement with that found above in the analysis of the behavior of the X_α line and it confirms the correctness of the interpretation of the origin to the X_δ and X_γ lines.

The Z_1 and Z_2 lines. These lines are resolved in the spectrum only in the no-phonon component. We have analyzed the case $\mathbf{P}\|\langle 112\rangle$. For small deformations the shift of the Z_1 and Z_2 lines to the long wavelength direction is the same as the shift of the long wavelength component of the α line and is considerably less than for the free exciton (the *FE* line). Consequently, the binding energy of these states of the EIC is sharply reduced and at least one of them (Z_2) becomes unstable with respect to decay into a free exciton and an impurity center in the ground states. Even at small uniaxial compression the Z_1 and Z_2 lines are strongly broadened and we were unable to detect the splitting of these lines. We note only that the identical shifts of the α line and the Z_1 and Z_2 lines towards long wavelength confirms that in the initial states of the EIC corresponding to the Z_1 and Z_2 lines both electrons are in the ground state Γ_1 and only one hole is in an excited state.

In the range $P = 200 - 500$ MPa it is very hard to follow the Z_1 line because of the appearance, in the no-phonon region of the spectrum, of emission lines associated with the recombination of EIC in the states $\{\Gamma^1_1\ \Gamma^3_1\ \Gamma^8_{5''}\}$ (Fig. 5). However, for $P > 500$ MPa and both for $\mathbf{P}\|\langle 112\rangle$ and $\mathbf{P}\|\langle 110\rangle$ there is observed in the no-phonon emission spectrum the Z^* line, which may be compared to the Z_1 line. We shall return to this question in the following section.

Splitting of EIC *levels in undeformed crystals resulting from electron-hole correlation*. It has been shown above that all the principal EIC emission lines can be explained within the framework of the one-electron approximation, in which interparticle interactions are neglected. It follows from group theory that additional splitting of the EIC levels due to interparticle interaction is possible only if there are at least two particles in unfilled shells (two different shells or a single shell). Consequently for the three lowest EIC states ($\{2\Gamma_1; \Gamma_{8,8',8''}\}$) additional splitting cannot occur. For an EIC with a single electron in the Γ_3 shell ($\{\Gamma_1, \Gamma_3; \Gamma_{8,8',8''}\}$) additional splitting can occur as a result both of electron-electron (e-e) exchange of Γ_1 and Γ_3 electrons—$(\Gamma_1 \times D_{1/2}) \times (\Gamma_3 \times D_{1/2}) = \Gamma_3 + \Gamma_4 + \Gamma_5$, and electron-hole ($e$-$h$) exchange of these electrons with a Γ_8 hole $(\Gamma_1 \times D_{1/2}) \times \Gamma_8 = \Gamma_3 + \Gamma_4 + \Gamma_5$, $\quad (\Gamma_3 \times D_{1/2}) \times \Gamma_8 = \Gamma_1 + \Gamma_2 + \Gamma_3 + 2\Gamma_4 + 2\Gamma_5$. Therefore one might expect additional fine structure in the δ, X_δ, and Y_δ lines. From Fig. 1 it can be seen that the halfwidths of these lines is somewhat greater than that of the α, X_α, *and* Y_α lines; however, the fine structure of these lines could not be resolved. The only additional structure that is apparent is that at the long wavelength edge of the δ line. Its origin is not understood. Thus, from Fig. 1 it can be seen that this structure disappears when the temperature is lowered to 2 K. Threfore we cannot exclude the possibility that it is associated with the recombination of an EIC in some other one-electron state, for example, $\{2\Gamma_1; (2p)\Gamma_{6,7}\}$.

Therefore we can conclude that the splitting of the states $\{\Gamma_1, \Gamma_3; \Gamma_{8,8',8''}\}$ is not greater than the halfwidths of the δ, X_δ, and Y_δ lines (0.4 meV).

§5. STRUCTURE OF EIC EXCITED STATES UNDER UNIAXIAL COMPRESSION OF THE CRYSTALS FOR LARGE DEFORMATIONS

From Fig. 6 it can be seen that the structure of the excited states of the EIC remains quite complicated also for highly compressed β-SiC crystals both for $\mathbf{P}\|\langle 110\rangle$, where two valleys remain in the conduction band, and for $\mathbf{P}\|\langle 112\rangle$, where the degeneracy is completely lifted in the electron and in the hole bands. The lowest excited state in both cases remains the hole $2p\Gamma^{8'}_{5'}$ state. The X_α emission line corresponds to this state. In β-SiC crystals compressed along the $\langle 110\rangle$ axis, with two valleys in the conduction band, the next excited state is the electron-only-excited state $\{\Gamma^1_1, \Gamma^3_2; \Gamma^8_{5'}\}$. The valley-orbit splitting of the electron $1s$ state is reduced, because of the decrease in the number of valleys, from 4.8 meV in the undeformed crystals (three valleys) to 3.6 meV in strongly compressed crystals (two valleys). This decrease in the magnitude of the valley-orbit splitting is in good agreement with the value expected in the

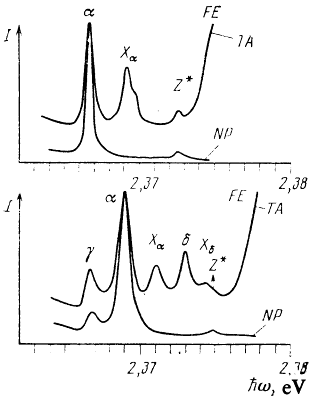

FIG. 6. *TA* and *NP* emission spectra of strongly compressed β-SiC crystals for $\mathbf{P}\|\langle 112\rangle$ (above) and $\mathbf{P}\|\langle 110\rangle$ (below). For the *TA* components of the spectrum the horizontal axis gives the total energy of the emitted photon and phonon.

framework of the one-electron approximation in the limit of very large deformations[19]: $(\Gamma_2^3-\Gamma_1^1)_{\mathbf{P}\|\langle 110\rangle} \approx 2/3(\Gamma_3-\Gamma_1)_{P=0}=3.2$ meV. We note also that in crystals highly compressed along the $\langle 110\rangle$ axis there remains in the *TA* spectrum the X_δ emission line, which corresponds to the recombination of an EIC in the electron- and hole-excited state $-\{\Gamma_1^1,\Gamma_2^3;(2p)\Gamma_{5'}^{8'}\}$ (Fig. 5).

In crystals compressed along the $\langle 112\rangle$ axis one valley remains in the conduction band. Therefore the energy of the electron-excited state Γ_1^3 gradually rises, both for a neutral donor and an EIC. This is reflected in the increase in the energy spacing between long wavelength components of the α and δ lines and the γ and δ lines, respectively (Figs. 3, 5). At large deformations ($P>500$ MPa) the $\{\Gamma_1^1,\Gamma_1^2;\Gamma_{5'}^8\}$ state becomes unstable and in the spectrum only the emission lines of the EIC in the ground electron state $(2\Gamma_1^1)$ remain. In this range of deformation the MEIC binding energy decreases sharply, and this leads to the disappearance of their emission lines (§7). It is interesting to note that the short wavelength components of the δ and γ lines, which components correspond to the recombination of the EIC in an excited state with holes $\pm 3/2(\Gamma)$ are still observed in the spectrum under conditions where the initial $\{\Gamma_1^1,\Gamma_1^3;\Gamma\}$ state is already unstable with respect to decay into a free exciton and an impurity in their ground states (Fig. 5). It is obvious that the lifetimes of these complexes must be sharply reduced. Therefore the δ^* and γ^* lines are strongly broadened with increasing deformation.

There is still another line that remains in the spectrum of the highly compressed crystals both for $\mathbf{P}\|\langle 112\rangle$ and $\mathbf{P}\|\langle 110\rangle$; this is the Z^* line. It is observed both in the no-phonon region of the spectrum as well as in the phonon replicas (Fig. 6). In both cases it was possible to trace this line reliably only for $P\gtrsim 500$ MPa, where it falls in the region of the spectrum that is free of other lines (on the long wavelength side of the α^* line, which corresponds to the recombination of the EIC in the state $\{2\Gamma_1^1;(1s)\Gamma_{5''}^8\}$). The α^* line has σ polarization (recombination of a hole with spin $\pm 3/2$) and the Z^* line has predominantly π polarization, i.e., it corresponds to the recombination of a hole with spin $\pm 1/2$. The difference in energy between the Z^* and α transitions under uniaxial compression of the crystals ($\sim 6.0\pm 0.2$ meV) (Fig. 5) is only slightly less that the energy difference of the Z_1 and α transitions in the undeformed crystals (~ 6.8 meV, Fig. 1). Therefore we associate the Z^* line with the recombination of a Γ_1^1 electron with a hole in the $2s$ state $\Gamma_{5'}^8$, having a spin $\pm 1/2$. In accordance with this interpretation it follows from the ratio of the intensities of the Z^* and α^* lines that the probability of the no-phonon transitions Z^* is considerably (about three times) smaller than that of the α^* transitions, which correspond to the recombination of holes in the $1s$ state.

For large deformations along the $\langle 112\rangle$ axis we were able to detect reliably in the *TA* spectrum still another weak line α^0, which is red shifted relative to the α line by more than 8 meV and which moves with increasing deformation towards long wavelengths almost twice as fast as the α line does (Fig. 5). We associate this line with the transition from the EIC ground state $\{2\Gamma_1^1;\Gamma_{5'}^8\}$ to the valley-orbit split state of the neutral donor $\{\Gamma_1^3\}$ (Fig. 2) since the energy spacing between the α and α^0 lines corresponds exactly to the difference in energy of the γ and δ transitions. The transition $\{2\Gamma_1;\ \Gamma_8\}\rightarrow\{\Gamma_3\}$ in undeformed crystals, within the framework of the shell model, is, as a one-electron transition, forbidden. Upon uniaxial compression of β-SiC crystals the transition $\{2\Gamma_1^1;\Gamma_{5'}^8\}\rightarrow\{\Gamma_1^3\}$ becomes resolved to the extent that the projection of the state Γ_1^3 onto Γ_1^1 becomes nonzero (the mixing of these states is due to the fact that they have the same symmetry). However, the probability of this transition remains rather small; it follows from experiment that $I(\alpha^0)/I(\alpha)\approx 10^{-2}$.

At small deformations we were not able to distinguish the α^0 line, since in this region of deformation it coincides with an E_2IC emission line. The dependence of the α^0 transition energy on P calculated from the spectral positions of the α, γ, and δ lines is shown in Fig. 5 by the dashed line.

§6. MULTIEXCITON-IMPURITY COMPLEXES IN UNDEFORMED CRYSTALS

Figure 7 shows the emission specta of β-SiC crystals for high excitation densities ($W\sim 1$ kW/cm^2) and various temperatures. From this figure it can be seen that, just as in the silicon crystals, the emission spectra in the *NP* and *TA* regions of the spectrum differ greatly because of the difference in the matrix elements M_{NP} and M_{TA} of the transition (§3).

The α lines. As mentioned in the introduction, the most intense emission lines in the no-phonon spectrum, $\alpha_1-\alpha_5$, have already previously[9,10] been associated with the recombination in MEIC's of electrons from the inner total valley-symmetric $1s\Gamma_1$ shell with $1s\Gamma_8$ holes. In other words, within the framework of the shell model these lines correspond to transition from the ground states E_mIC$\{2\Gamma_1,(m-1)\Gamma_3; m\Gamma_8\}$ to the electron-excited states E_{m-1}IC$\{\Gamma_1, (m-1)\Gamma_3;(m-1)\Gamma_8\}$, $(m\geqslant 4)$ (Fig. 8). In the five-exciton complex the fifth hole must fall into the next shell beyond Γ_8, since the Γ_8 state is only fourfold degenerate. Therefore the α_5 line must correspond to the transition from the $\{2\Gamma_1, 4\Gamma_3;$

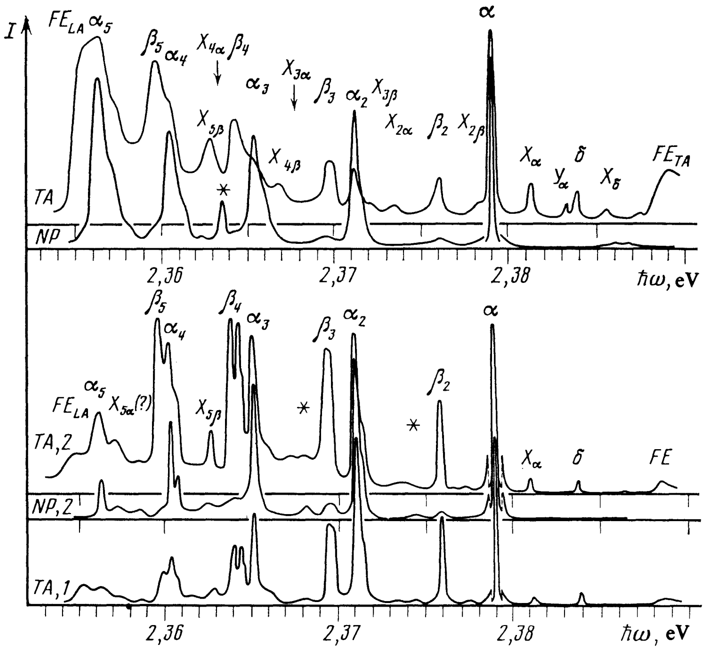

FIG. 7. Emission spectra of MEIC in β-SiC at two temperatures, 1.8 K (above) and 20 K (below) without phonon emission (NP) and with emission of a TA phonon (TA) for high excitation densities. For the TA spectrum curve 1 was recorded at $W = 500\ \mathrm{W/cm^2}$; the rest of the spectra for $W = 1500\ \mathrm{W/cm^2}$. For the TA components of the spectrum the horizontal axis gives the total energy of the emitted photon and phonon. The asterisks indicate the emission lines due to the presence of other residual impurities in the B-SiC.

$4\Gamma_8, \Gamma_X\}$ state into the $\{\Gamma_1, 4\Gamma_3; 3\Gamma_8, \Gamma_X\}$ state, which is both electron- and hole-excited. For the α_1 and α_2 lines this interpretation is in accord with the previously determined[9] splitting of these lines in a magnetic field.

The β lines. The question of the β emission lines of MEIC in β-SiC still remains open. The $1s\Gamma_1$ state for electrons is already filled in the EIC, while in the MEIC, according to the shell model, the electrons must occupy the valley-antisymmetric $1s\Gamma_3$ electron shell, which follows next after the $1s\Gamma_1$ and is fourfold degenerate taking into account the spin.[5] Since the wave function of the Γ_3 electrons vanishes at $r = 0$, the probability of no-phonon transitions involving these electrons is small.[2] However, in the TA region of the spectrum the intensities of the corresponding so-called β transitions $\{2\Gamma_1, (m-1)\Gamma_3; m\Gamma_8\} \rightarrow \{2\Gamma_1, (m-2)\Gamma_3; (m-1)\Gamma_8\}$ $(m = 2-4)$, (Fig. 8) should be comparable with the intensities of the α transitions. In the five-exciton complex $\{2\Gamma_1, 4\Gamma_3; 4\Gamma_8, \Gamma_X\}$ the recombination of Γ_3 electrons is possible both with a Γ_8 hole (the β_5 transition) and with a Γ_X hole (we designate this the $X_{5\beta}$ transition, Fig. 8). The $\beta_2 - \beta_4$ transitions and the $X_{5\beta}$ transition (Fig. 8) correspond to transitions between the ground states of the complexes with $(m-1)$ bound excitons. From Fig. 7 it can be seen that in the TA region of the spectrum the most intense line next to the α_m line is the β_m line. From an analysis of the behavior of the MEIC emission spectra with the emission of a TA phonon, as the excitation density and the temperature are varied over wide limits, it follows that in all cases the intensity ratios remain unchanged for the following pairs of lines: α_2–β_2, α_3–β_3, and α_4–β_4, and the triplet of lines α_5, α_5 and $X_{5\beta}$. As the index increases from two to five the intensity ratio $I(\beta_m)/I(\alpha_m)$ increases monotonically: it is equal roughly to 1/2, 2/2, 3/2, and 4/2 for $m = 1, 2, 3,$ and 4 (Fig. 7), i.e., it corresponds to the ratio of the number of Γ_3 electrons to the number of Γ_1 electrons in the MEIC. Thus, these results show that it is the β_m lines that correspond to the recombination of Γ_8 holes with Γ_3 electrons in the MEIC.

Let us now turn to the no-phonon component. From Fig. 7 it can be seen that in this component the intensity of

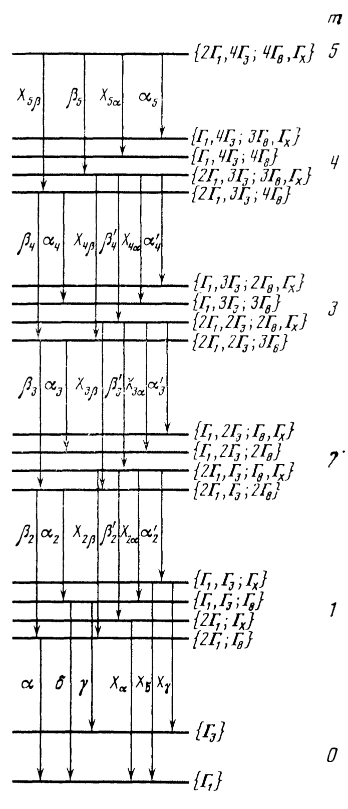

FIG. 8. Energy level diagram of MEIC bound to nitrogen atoms and the resolved one-electron transitions between them in β-SiC; $\Gamma_X = 2p\Gamma_8$.

the β lines is about two orders of magnitude less than that of the α lines. Nonetheless, this intensity ratio $I(\beta_m)/I(\alpha_m)$ in β-SiC is about two orders of magnitude greater than for Si, where it is $\lesssim 10^{-4}$ (Ref. 6). The actual value of $I(\beta_m)/I(\alpha_m)$ is determined by the ratio of the constants $\tilde{\eta}$ and $\tilde{\lambda}$ in the selection rule for transitions with scattering by the impurity potential.[16]. For recombination of Γ_1 electrons (the α line) $I_{NP} \sim (2\tilde{\eta} + \tilde{\lambda})^2$ and for recombination of Γ_3 electrons (the β line) $I_{NP} \sim 2(\tilde{\eta} - \tilde{\lambda})^2$. From the experimental values of $I_{NP}(\beta_m)/I_{NP}(\alpha_m) \approx 0.01$ we estimate that in β-SiC $\tilde{\lambda} = 0.8\tilde{\eta}$ (as compared to $\tilde{\lambda} = 0.98\tilde{\eta}$ in silicon).

The $X_{5\beta}$ transition in E_5IC. As noted above, in E_5IC the fifth hole goes into a new shell Γ_X. In the emission spectrum of this complex there should be two new lines (compared to an MEIC with fewer bound excitons) which correspond to the recombination of Γ_X hole with Γ_1 and Γ_3 electrons (Fig. 8). Experimentally for E_5IC only one of the extra lines $X_{5\beta}$, has been reliably observed, and only in the phonon replicas. The ratio of the $X_{5\beta}$ and β_5 line intensities is $I(X_{5\beta})/I(\beta_5) \approx 1/4$, which indicates that this line corresponds to the recombination of a Γ_3 electron with a Γ_X hole. Within the framework of this interpretation the difference in energy between the Γ_8 and Γ_X hole states in E_4IC is equal to the difference in energy between the $X_{5\beta}$ and β_5 transitions (Fig. 8), i.e., it should be about 3 meV. This value is close to the energy difference between the $1s\Gamma_8$ and $2p\Gamma_{8'}$ hole states in the ordinary EIC [$\approx$2.2 meV (§3)]. It can therefore be assumed that the fifth hole goes into the fourfold degenerate $2p\Gamma_{8'}$ state and the ground state of E_5IC can be written in the form $\{2\Gamma_1, 4\Gamma_3; 4\Gamma_8, (2p)\Gamma_{8'}\}$. Three out of the four possible E_5IC one-electron transitions α_5, β_5, and $X_{5\beta}$ are readily visible in the spectrum (Figs. 7 and 8). The probability of the other transitions $X_{5\alpha}$, which corresponds to the recombination of a Γ_1 electron with a $2p\Gamma_{8'}$ hole (Fig. 8) is considerably smaller than that of the β_5 transition because of the small number of Γ_1 electrons and $2p\Gamma_8$ holes in E_5IC. As in the case of the EIC X_α emission line, the $X_{5\alpha}$ line should be observed only in the phonon replicas. It is possible that the transition $X_{5\alpha}$ corresponds to the weak line $X_{5\alpha}$ (?) near the intense β_5 line.

The MEIC *binding energy*. From the analysis of the MEIC emission lines presented above we can determine uniquely the structure of the MEIC and EIC ground states and the diagram of the resolved transitions between them (Fig. 8). From the spectral position of the α, $\beta_2 - \beta_4$ and $X_{5\beta}$ emission lines and of the emission line of the free exciton (FE) we have found with the use of this diagram the binding energies Δ_m of the MEIC excitons, and from the positions of the α_m and β_m lines the energy spacings between the ground and electron-excited EIC and MEIC states. These values are given in Table I. From the table it can be seen that the binding energies of excitons in complexes bound to nitrogen in β-SiC increase monotonically with the number of bound excitons. In E_2IC and E_5IC, in which new shells begin to fill (the $1s\Gamma_3$ electron shell in E_2IC and the $2p\Gamma_8$ hole shell in E_5IC), the binding energy increase is relatively small.

Let us turn now to a consideration of the change in the MEIC emission spectra that occurs with increasing temperature (Fig. 7). Here one should note two specific features in comparison to the behavior of MEIC in silicon crystals. First, there is the strong increase with no fall-off at high temperatures ($T \sim 20$ K) in the relative intensities of the emission lines of the complexes having a large number of bound excitons. Second, there is the very weak dependence on excitation density of the relative emission line intensities of the MEIC at high temperatures as the excitation density is varied over three orders of magnitude. [At low temperatures, as in Si, the relative β-SiC MEIC emission line intensities depend strongly on the excitation density (Fig. 7)]. The observed behavior of the MEIC emission spectra in β-SiC at 20–30 K can be explained if we assume that in the MEIC plus free excitons system thermal quasiequilibrium is attained and if we bear in mind that the MEIC binding energy in β-SiC is substantially (3–4 times) larger than in Si. As the temperature is lowered the decrease in the rate of thermal evaporation of excitons from the complexes and the sharp decrease

TABLE I. Binding energy (Δ_m) and energy distance btween the various electron and hole terms in the complexes bound to nitrogen atoms in β-SiC. [$E_{gx} = (2.3881 \pm 0.0001)$ eV (Ref. 21).]

	Number of bound excitons	0	1	2	3	4	5
$P=0$	Δ_m, meV 1)	–	9,0±0,2	12,1	18,7	23,7	26,3
P∥⟨110⟩	Δ_m, meV	–	8,2±0,3	12,1	16,0	–	–
	electrons :						
$P=0$	$\Gamma_3-\Gamma_1$, meV	8,3	4,8	4,2–4,5	3,7–4,1	3,6	–
P∥⟨112⟩	$\Gamma_2{}^3-\Gamma_1{}^3$, meV	–	–	2,6	–	–	–
P∥⟨110⟩	$\Gamma_2{}^3-\Gamma_1{}^1$, meV	5,9	3,6	2,8	2,4	–	–
	holes :						
$P=0$	$2p\Gamma_{8'}-1s\Gamma_8$, meV	–	2,2 1,8 3)	2,3	2,5	2,9	–
P∥⟨112⟩	$2p\Gamma^{8'}_{5'}-1s\Gamma^{8}_{5'}$, meV	–	2,5–3,0	4,0 3,6 2)	– 3,5 2	– 3,5 2)	–
P∥⟨110⟩	$2p\Gamma^{8'}_{5'}-1s\Gamma^{8}_{5'}$, meV	–	2,2	– 2,5 2)	– 2,5 2)	– 2,5 2)	– –

Notation: 1) Δ_m is the minimum energy required for the removal of one exciton from the complex. 2) In the first electron-excited state (Γ_1, Γ_3). 3) In the first hole-excited state.

in the concentration of free excitons increase the time of redistribution of the excitons among the MEICs and this, in turn, results in the situation where the MEIC system, which has a finite lifetime, is far from thermodynamic equilibrium.

Transitions from MEIC *excited states*. At high temperatures, because of the increase in the MEIC excited state population, the additional recombination radiation lines should grow in the emission spectrum. Actually, it can be seen from Fig. 7 that there are $X_{2\alpha}$, $X_{2\beta}$, $X_{3\beta}$, and $X_{4\beta}$ lines in the spectrum. These increase in size only in the phonon replicas. The energy spacing between the β_m and $X_{m\beta}$ lines is 2.5–3 meV, i.e., it is close to the difference in the energy of the holes in the $1s\Gamma_8$ and $2p\Gamma_{8'}$ shells for both the EIC and E_4IC. Therefore we can suppose that these lines correspond to the recombination of $2p\Gamma_{8'}$ holes with $1s\Gamma_3$ electrons, i.e., they correspond to the transitions from the $\{2\Gamma_1, (m-1)\Gamma_3; (m-1)\Gamma_8, (2p)\Gamma_{8'}\}$ E_mIC excited states to the E_{m-1}IC ground state ($m \leqslant 4$) (Fig. 8). In the case of the recombination of E_5IC having a $2p\Gamma_{8'}$ hole in the ground state the $X_{5\beta}$ transition, as noted above, is observed also at $T = 1.8$ K (Fig. 7). In accordance with the MEIC level diagram shown in Fig. 8, the energy differences of the E_5IC $X_{5\beta}$ and β_5 lines and the $X_{4\beta}$ and $\beta_4 E_4$IC emission lines coincide (they are both equal to the difference between the $2p\Gamma_{8'}$ and $1s\Gamma_8$ energy terms in the E_4IC). The values obtained for the differences between the $2p\Gamma_{8'}$ and $1s\Gamma_8$ energy terms for various MEIC's are given in Table I.

We shall now examine other possible transitions from the MEIC $\{2\Gamma_1, (m-1)\Gamma_3; (m-1)\Gamma_8, (2p)\Gamma_{8'}\}$ excited states (Fig. 8). There are three: the α' transitions to the $\{\Gamma_1, (m-1)\Gamma_3; (m-2)\Gamma_8, (2p)\Gamma_{8'}\}$ states, the β' transitions to the $\{2\Gamma_1, (m-2)\Gamma_3; (m-2)\Gamma_8, (2p)\Gamma_{8'}\}$ states, and the $X_{m\alpha}$ transitions to the $\{\Gamma_1, (m-1)\Gamma_3; (m-1)\Gamma_8\}$ states. The energies of the β' transitions can be calculated from the given energy values of the X_β transitions and the energy differences of the $1s\Gamma_8$ and $2p\Gamma_{8'}$ MEIC hole terms (Table I). As is expected within the framework of the shell model the energies of the β' transitions are close to those of the β transitions and because of the large halfwidths of the emission lines in the *TA* component of the spectrum they are not resolved out of the background of the more intense β lines. In exactly the same way the energies of the α' transitions should be close to those of the α transitions. It can be seen from Fig. 7 that at the α lines in the no-phonon spectrum there are short-wavelength satellites which are shifted towards the short-wavelength region of the spectrum relative to the α lines by only 0.2–0.4 meV. Because of the large relative intensities of these satellites at $T = 2$ K, where the excited states of the MEIC, judging from intensities of the $X_{m\alpha}$ lines, are almost unoccupied, it is evidently not possible to associate them with the α' transitions. However, it is still possible that at high temperatures the contribution from the α' transitions is appreciable. For instance at temperatures of 20–30 K, where kT is considerably greater than 0.2–0.4 meV, a clearly discernable increase in the relative intensities of the short wavelength satellites of the α line is observed.

The spectral positions of the $X_{m\alpha}$ lines can also be determined by using the diagram in Fig. 8 and taking into account the coincidence in the energies of the α and α' transitions. These positions are shown by the arrows in Fig. 7. In the spectrum only the $X_{2\alpha}$ line is well resolved, while the $X_{3\alpha}$ and $X_{4\alpha}$ lines are lost in the edges of the intense $X_{4\beta}$ and $X_{5\beta}$ lines, respectively.

Splitting of the states by the interparticle interaction. Up until now we have not taken into account the fine structure of the emission lines and have discussed the results within the framework of the one-electron shell model. From Fig. 7 it can be seen that the emission lines, particularly in the *TA* region of the spectrum, have a rather large halfwidth and in the majority of the cases their fine structure is not resolved. Nevertheless, in Fig. 7 the relatively large doublet splitting of the β_3 and β_4 lines is evident. The relative intensities of the components in these doublets is independent of the excitation density and the temperature. As the temperature is increased only a broadening of the individual components is observed, and for $T > 15$ K they are no longer resolved.

The β_3 and β_4 lines, as we have determined above, correspond, respectively, to the $\{2\Gamma_1, 3\Gamma_3; 4\Gamma_8\} \rightarrow \{2\Gamma_1, 2\Gamma_3; 3\Gamma_8\}$ and $\{2\Gamma_1, 2\Gamma_3; 3\Gamma_8\} \rightarrow \{2\Gamma_1, \Gamma_3; 2\Gamma_8\}$ transitions. In all these MEIC states the Γ_1 shell for electrons is completely full. Therefore the (e–e) interaction can be important only in the Γ_3 shell (taking into account the Γ_3 electrons ($\Gamma_3 \times D_{1/2}$) have Γ_8 symmetry); the (h–h) interaction in the Γ_8 shell and the (e–h) interaction between the Γ_3 electrons and the Γ_8 holes are important.[16] The e–e and h–h interactions can cause a splitting of only the $2\Gamma_3$ and $2\Gamma_8$ states, respectively, since each of the rest of the states, namely, Γ_8 $\Gamma_8 \times \Gamma_8 \times \Gamma_8 \rightarrow \Gamma_8$ and $\Gamma_8 \times \Gamma_8 \times \Gamma_8 \times \Gamma_8 \rightarrow \Gamma_1$ (here we take the Pauli principle into account) are irreducible. In a similar way we find that the e–h exchange leads to additional level splitting only in complexes with simultaneously unfilled electron and hole shells. Among the ground states these include the states $\{2\Gamma_1, \Gamma_3; 2\Gamma_8\}$ (E_2IC) and $\{2\Gamma_1, 2\Gamma_3; 3\Gamma_8\}$ (E_3IC).

From Fig. 7 it can be seen that the E_2IC β emission line (β_2) corresponding to the $\{2\Gamma_1, \Gamma_3; 2\Gamma_8\} \rightarrow \{2\Gamma_1; \Gamma_8\}$ transition is practically unsplit, as is the EIC emission line corresponding to the transition from the excited state $\{\Gamma_1, \Gamma_3; \Gamma_8\}$ to the ground state of the neutral donor $\{\Gamma_1\}$ (the δ line). Therefore it should be supposed that neither e–h nor h–h exchange are dominant. Consequently, it is the e–e exchange that is most important in MEIC bound to donors in β-SiC. It leads to the splitting of the E_3IC ground state $\{2\Gamma_1, 2\Gamma_3; 3\Gamma_8\}$, which is the final state for the β_4 transition and the initial state for the β_3 transition (Fig. 8). From Fig. 7 it can be seen that the splitting of the β_3 and β_4 lines is not mirror symmetric; therefore it is not possible to ignore completely e–h exchange. The electron-hole interaction of Γ_1 and Γ_3 electrons with Γ_8 holes as well as the electron-electron interaction of Γ_1 and Γ_3 electrons in MEIC leads also to a weak splitting of the α_m line. It can be seen from Fig. 7 that two main components can be discerned in all these lines. In a more thorough description of the spectra of some crystals additional structure appears. However, we were not able to resolve fully this structure. In order of magnitude, as seen in Fig. 7, the splitting of the α_m line does not exceed 0.3 meV for E_2IC and 0.6 meV for E_4IC.

Previously, the interparticle interaction in MEIC has been studied for the cases of EIC and E_2IC bound to substitutional donors in silicon.[7,8] It was found that in these complexes the strongest splitting of the one-electron states was due to *e–h* exchange. However, in the investigations of complexes with one and two bound excitons the authors were able only to estimate the *e–e* exchange of Γ_1 and Γ_3 electrons in the $\{\Gamma_1, \Gamma_3; \Gamma_8\}$ state. From calculations, carried out for the case of Si (Ref. 24), for the energies of EIC bound to donors it follows that the splitting of the $2\Gamma_3$ electron state should be considerably greater than that of the $\{\Gamma_1, \Gamma_3; \Gamma_8\}$ state because of both *e–e* and *e–h* exchange. This conclusion is in good agreement with the results we have obtained in the investigation of E_3IC in β-SiC.

The additional satellites of the α_5 line (the transition $\{2\Gamma_1, 4\Gamma_3; 4\Gamma_8, (2p)\Gamma_{8'}\} \rightarrow \{\Gamma_1, 4\Gamma_3; 3\Gamma_8, (2p)\Gamma_{8'}\}$) can be associated only with interparticle interaction in the E_4IC excited state (*e–h* exchange of a Γ_1 electron with $1s\Gamma_8$ or $2p\Gamma_{8'}$ holes and *h–h* exchange of $1s\Gamma_8$ and $2p\Gamma_{8'}$ holes). As was found above, the *e–h* exchange of a Γ_1 electron and a $1s\Gamma_8$ hole is quite small. Therefore we can suppose that the important interaction is the exchange interaction of electrons with $2p\Gamma_8$ holes or *h–h* exchange.

§7. MEIC IN STRONGLY COMPRESSED CRYSTALS

The high stability of MEIC in indirect-gap semiconductors is related to the degeneracy of the electron and hole bands.[2] At small deformations of the crystal there is a rather complicated splitting observed for the emission lines of the complexes that is due to the splitting of both the electron and hole bands. An analysis of this splitting, in many respects similar to that carried out previously in different papers for MEIC in silicon,[16] permits us to verify the energy level diagram of MEIC in β-SiC presented above (Fig. 8). While not dwelling at length on this analysis (see Ref. 25), we note that the splitting of all the lines ($\alpha_1 - \alpha_5, \beta_2 - \beta_3$, and $X_{5\beta}$) is in good agreement with that expected within the framework of the shell model and the MEIC level diagram shown in Fig. 8.

Strong uniaxial compression of the β-SiC crystals leads to a partial or complete lifting of the orbital degeneracy of the bands. As expected within the framework of the shell model, when the orbital degeneracy of both bands is completely lifted ($\mathbf{P}\|\langle 112\rangle$) the emission lines of all the complexes except the EIC disappear from the spectrum. However, in the case of uniaxial compression of β-Sic crystals along the $\langle 110\rangle$ axis, where the orbital degeneracy is lifted only in the valence band while two valleys remain in the conduction band, emission lines of complexes with one, two, and three bound excitons remain in the spectrum up to the very highest deformations (Fig. 9). Since, for $P \gtrsim 500$ MPa the relative intensities of the emission lines of the various complexes do not depend on the deformation for constant temperature and excitation density, we can conclude that their binding energies at such deformations are independent of P.

The structure of E_2IC in highly compressed β-SiC crystals as well as in uniaxially compressed silicon crystals with two valleys in the conduction band ($\mathbf{P}\|\langle 100\rangle$) are simple: two holes fill completely the ground state $1s$ shell $\Gamma^8_{5'}$; of the three electrons two occupy the completely valley-symmetric state Γ^1_1 and the third electron goes into the Γ^3_2 shell, which is antisymmetric with respect to two valleys and doubly spin-degenerate (see the insert in Fig. 3). Accordingly, in the E_2IC emission spectrum two lines are observed, α_2 and β_2, which correspond, respectively, to the recombination of $\Gamma^8_{5'}$ holes with Γ^1_1 and Γ^3_2 electrons. The β_2 line, as expected, is seen only in the phonon replicas. From its position it is possible to determine the E_2IC binding energy. From Figs. 7 and 9

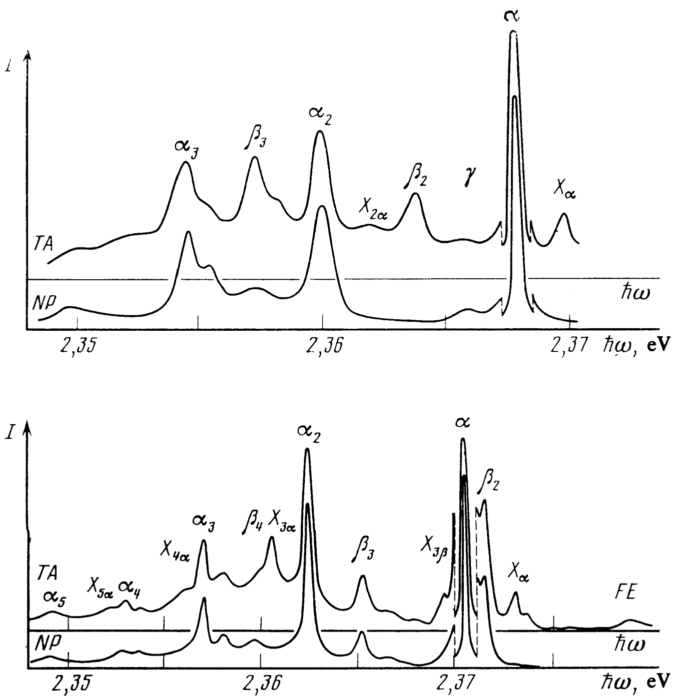

FIG. 9. Emission spectra of MEIC in β-SiC crystals strongly compressed along the $\langle 110\rangle$ axis (above, $P = 800$ MPa) and $\langle 112\rangle$ axis (below, $P = 500$ MPa) for $T = 4.3$ K in the *NP* and *TA* regions of the spectrum; $W = 1200$ W/cm^2. For the *TA* component the horizontal axis gives the total energy of the emitted photon and phonon.

TABLE II. Binding energy of EIC and the excited states of EIC in undeformed and strongly compressed β-SiC crystals. All energies in meV. The states $\Gamma^8_{5'}$ correspond to spin 1/2 and $\Gamma^8_{5''}$ to spin 3/2.

State (group T_d)	$P=0$	State (group C_{2v})	$\mathbf{P} \parallel \langle 110 \rangle$	$\mathbf{P} \parallel \langle 112 \rangle$
Binding energy	9,0±0,2	—	8,0±0,2	7,6±0,2
$\{2\Gamma_1; (2p)\Gamma_{8'}\}$	2,2±0,1	$\{2\Gamma^1_1; (2p)\ \Gamma^{8'}_{5'}\}$	2,2±0,2	2,5±0,2
		$\{2\Gamma^1_1; (2p)\ \Gamma^{8'}_{5''}\}$	2,2±0,2	3,0±0,2
$\{2\Gamma_1; (2p)\Gamma_{8''}\}$	4,0±0,1	—	—	—
$\{2\Gamma_1; (2s)\Gamma_8\}$	6,8±0,1	$\{2\Gamma^1_1; (2s)\ \Gamma^8_{5'}\}$	5,8±0,2	6,0±0,2
$\{\Gamma_1, \Gamma_3; \Gamma_8\}$	4,8±0,1	$\{\Gamma^1_1, \Gamma^3_2; \Gamma^8_{5'}\}$	3,6±0,2	—
$\{\Gamma_1, \Gamma_3; (2p)\Gamma_{8'}\}$	(4,8+1,8)±0,3	$\{\Gamma^1_1, \Gamma^3_2; (2p)\ \Gamma^{8'}_{5'\ (5'')}\}$	(3,6+2,0)±0,3	—

it can be seen that, as in silicon, the energy is almost independent of the magnitude of the uniaxial deformation.

In the three-exciton-impurity complex, four electrons fill completely both $1s$ shells Γ^1_1 and Γ^3_2. Of the three holes, two completely fill the ground state hole shell $1s\Gamma^8_{5'}$, and the third must go into a higher shell. From the preceding analysis (§5) of the energy spectra of the holes in the EIC under uniaxial compression of the crystals it follows that these hole states may be $2p\Gamma^{8'}_{5'}$, the energy of which is almost independent of the deformation. It is obvious that besides the two emission lines corresponding to the recombination of Γ^1_1 and Γ^3_2 electrons with $1s\Gamma^8_{5'}$ holes (α_3 and β_3) there should appear in the E_3IC emission spectrum at high P two more lines (only in the phonon replicas), corresponding to the recombination of these electrons with a $2p\Gamma^{8'}_{5'}$ hole ($X_{3\alpha}$ and $X_{3\beta}$). From Fig. 9, however, it is seen that these spectrally resolved lines cannot be distinguished in the MEIC emission spectrum. The short-wavelength satellites of the α_3 and β_3 lines cannot be associated with the $X_{3\alpha,\beta}$ transitions, since the short wavelength satellite of the α_3 line is also observed in the no-phonon component (Fig. 9). However, we call attention to the fact that the energy spacings between the α_3 and β_3 lines and the β_3 and α_2 lines are close to the energies of the holes in the $2p\Gamma_{8'}$ states in the EIC (the X_α line) and in the E_2IC (the $X_{2\alpha}$ line). Therefore the possibility is not excluded that the $X_{3\alpha}$ and $X_{3\beta}$ lines coincide with the β_3 and α_2 lines, respectively. That this is indeed so can be easily seen from an analysis of the E_3IC emission spectra in crystals compressed along the $\langle 112 \rangle$ axis. In this case the energy of the lowest excited state $1s\Gamma^3_1$ of the neutral donor increases with increasing deformation (see the insert in Fig. 3). As a result, the energy of the transition β_3 and the energy spacing between the β_3 line and the α_3 and α_2 lines depend on the amount of deformation. It can be seen from Fig. 9 that in the emission spectrum of crystals compressed along the $\langle 112 \rangle$ axis, for intermediate deformations both lines associated with the recombination of a $2p\Gamma^{8'}_{5'}$ hole are well resolved. The energy difference for the $X_{3\alpha}$ and α_3 ($X_{3\beta}$ and β_3) transitions is ~ 3.5 meV and it does not depend on the magnitude of the deformation. Thus we can conclude that under strong compression of crystals with a valence band splitting greater than 3.5–4 meV the third hole in E_3IC goes into the $2p\Gamma^{8'}_{5'}$ shell. In this case in β-SiC crystals compressed along the $\langle 110 \rangle$ axis the E_3IC binding energy decreases by an amount equal to the energy difference between the $1s\Gamma_8$ and $2p\Gamma_{8'}$ hole states (Table I).

§8. CONCLUSIONS

On the basis of the investigation of the emission spectra of lightly doped β-SiC crystals for various temperatures and excitation densities, and with the use of uniaxial compression of the crystals, we have succeeded in deciphering the complex structure of the states of both the ordinary EIC and the MEIC's with 2–5 bound excitons. This structure proved to be considerably more complicated that for the Si crystals, but the main properties of the complexes, as in the case of Si, are quite well described within the framework of the one-electron shell model. An important feature of the complexes in β-SiC is the very small energy of the $2p$ hole states. The principal energy parameters of the EIC and MEIC levels are shown in Tables I and II. As seen from these tables even the states of an EIC simultaneously containing an electron and hole in the excited states have a comparatively large binding energy in β-SiC. We note also that when the conduction band is degenerate the MEIC binding energy does not decrease when the hole $2p$ shell begins to be occupied.

From an analysis of the fine structure of the MEIC emission lines it follows that the *e–e* exchange of electrons in the Γ_3 shell produces the most important splitting of the one-electron states. A feature of the MEIC's in β-SiC is the appearance of the additional satellites of the α and β emission lines of the MEIC's containing a hole in the $2p$ states. To determine the nature of the splitting of the one-electron states of the MEIC's in these complexes requires additonal investigations.

In conclusion the authors express their deep gratitude to N. K. Prokof'ev for kindly providing the crystals, to I. S. Gorban', and S. I.Gubarev, I. V. Kukushkin, A. V. Malyavkin, and V. B. Timofeev for helpful discussions, and to I. E. Itskevich for help in carrying out the experiments.

[1)] For the case of uniaxial compression of the crystals, the upper index denotes the initial state in the undeformed crystal.

[1]A. S. Kaminskiĭ, Ya. E. Pokrovskiĭ, and N. V. Alkeev, Zh. Éksp. Teor. Fiz. **59**, 1937 (1970) [Sov. Phys. JETP **32**, 1048 (1971)].
[2]G. Kirczenow, Canad. J. Phys. **55**, 1787 (1977).
[3]M. L. W. Thewalt, Canad. J. Phys. **55**, 1463 (1977).
[4]V. D. Kulakovskii, Pis'ma Zh. Eksp. Teor. Fiz. **27**, 217 (1978) [JETP Lett. **27**, 202 (1978)].
[5]G. L. Bir and G. E. Pikus, Simmetriya i deformatsionnye effekty v poluprovodnikakh (Symmetry and deformation effects in semiconductors) Nauka, Moscow (1972).
[6]M. L. W. Thewalt in: Excitons, ed: M. D. Sturge, and I. I. Rashba, North-Holland, Amsterdam (1983).
[7]A. S. Kmainskiĭ, V. A. Karasyuk and Ya. E. Pokrovskiĭ, Pis'ma Zh. Eksp. Teor. Fiz. **33**, 141 (1982) [Sov. Phys. JETP **33**, 132 (1981)].
[8]A. S. Kaminskiĭ, V. A. Karasyuk, and Ya. E. Lokrovskiĭ, Zh. Eksp. Teor. Fiz. **83**, 2237 (1982) [Sov. Phys. JETP **56**, 1295 (1982)].
[9]P. J. Dean, D. C. Herbert, D. Bimberg, and W. J. Choyke, Phys. Rev. Lett. **37**, 1635 (1976).
[10]D. C. Herbert, P. J. Dean, and W. J. Choyke, Solid State Commun. **24**, 383 (1977).
[11]R. L. Hartman and P. J. Dean, Phys. Rev. **B2**, 951 (1970).
[12]A. E. Mayer and E. C. Lightowlers, J. Phys. C **12**, L539, L945 (1978).
[13]G. E. Pikus and N. S. Averkiev, Pis'ma Zh. Eksp. Teor. Fiz. **32**, 352 (1980) [JETP Lett. **32**, 328 (1980)].
[14]A. E. Mayer and E. C. Lightowlers, J. Luminesc. **24/25**, 389 (1981).
[15]V. D. Kulakovskiĭ, A. V. Malyavkin, and V. B. Timofeev, Zh. Eksp. Teor. Fiz. **76**, 272 (1978) [Sov. Phys. JETP **49**, 139 (1979)].
[16]V. D. Kulakovskiĭ, G. E. Pikus, and V. B. Timofeev, Usp. Fiz. Nauk **135**, 237 (1981) [Sov. Phys. Usp. **24**, 815 (1981)].
[18]Yu. A. Vakulenko, I. S. Gorban', V. A. Gubanov, and A. A. Pletyushkin, Fiz. Tverd. Tela (Leningrad) **26**, 3555 (1984) [Sov. Phys. Solid State **26** 2139 (1984)].
[19]G. L. Bir and G. E. Pikus, op. cit., p. 584.
[20]S. R. Pfeiffer and H. B. Shore, Phys. Rev. **B25**, 3897 (1982).
[21]I. S. Gorban', V. A. Gubanov, V. G. Lysenko, A. A. Pletyushkin, and V. B. Timofeev, Fiz. Tverd. Tela (Leningrad) **26**, 2282 (1984) [Sov. Phys. Solid State **26**, 1385 (1984)].
[22]R. L. Jones and P. Fisher, Phys. Rev. **B2**, 2016 (1970).
[23]A. Onton, P. Fisher, and A. K. Ramdas, Phys. Rev. **163**, 686 (1967).
[24]G.-C. Chang and T. C. McGill, Phys. Rev. **B25**, 3945 (1982).
[25]V. A. Gubanov and V. D. Kulakovskiĭ, Contributed paper to the meeting "Excitons 84," Fiz. Tverd. Tela (Leningrad) **27**, 5 (1985) [*sic*].

Tanslated by J. R. Anderson